HARMONIC EMISSION LEVEL ASSESSMENT CONSIDERING THE INFLUENCE OF FILTERS IN HARMONIC SOURCE SIDE

Qian FENG
State Grid Shanghai Electric power research institute-China
2653687386@qq.com

Mu CUO
State Grid Tibet Electric power research institute-China
cuomu5263@163.com

Xinggang YANG
State Grid Shanghai Electric power research institute-China
yangxingang@sh.sgcc.com.cn

Jinshuai ZHAO
Sichuan University-China
Jinshuai_zhao_scu@163.com

Fangwei XU
Sichuan University -China
xufangwei@scu.edu.cn

Hongru ZHENG
Sichuan University -China
1246815421@qq.com

ABSTRACT

Evaluation of the harmonic emission levels for a harmonic source at the point of common coupling (PCC) is of major significance for harmonic mitigation. Traditional emission level evaluation methods are based on the assumption that the target harmonic source side impedance (Z_H) *is far higher than the utility side impedance* (Z_U). *Therefore, only* Z_U *must be calculated during the evaluation process. This assumption is satisfactory for general industrial nonlinear loads. However, for situations in which harmonic filters have been installed on the target harmonic source side,* Z_H *is reduced and may not be far greater than* Z_U *at certain frequencies. In this situation, it is then necessary to obtain the harmonic impedances for both sides at the PCC. However, most existing methods can only calculate* Z_U. *To solve this problem, the complex independent component analysis (ICA) method, which is a widely-known algorithm in this field, is improved in this paper to assess the harmonic emission level accurately when the amplitude of* Z_H *is not much higher than that of* Z_U. *First, a sparse component analysis is introduced into the traditional complex ICA to screen the local signals which are strongly consistent with the true harmonic source signals. Subsequently, a screening mechanism is proposed to screen the local signals again with the objective of non-Gaussian maximization. Finally, using the local signals that are obtained from the two screening processes, we can calculate the harmonic impedances of both sides at the PCC accurately and also evaluate the harmonic emission level.*

INTRODUCTION

With the widening use of power electronics, harmonic pollution is becoming an increasingly serious problem [1]. Evaluation of the harmonic emission level for each harmonic source has guiding significance for mitigation of harmonics.

When assessing the harmonic emission level of a harmonic source at the point of common coupling (PCC), we often divide the complete system into a target harmonic source side and a utility side. Traditional assessment methods assume that the harmonic impedance of the target harmonic source side (Z_H) is far greater than that of the utility side (Z_U). Therefore, the influence of Z_H on the assessment process can be ignored and only Z_U must be calculated [2-5]. This assumption holds for general nonlinear loads. However, the existing studies neglect the situation where harmonic filters are installed in the target harmonic source side, which would mean that Z_H may be reduced and the above important assumptions would not then hold.

Calculation of the harmonic impedances is important for evaluation of the harmonic emission level. Widely-used harmonic impedance calculation methods include the fluctuation method, the regression method, the covariance characteristic method, and the independent component method. Among these methods, the fluctuation [6] and regression [7] methods are mainly suitable for situations with stable background harmonics. To reduce the interference caused by background harmonic fluctuations, a method based on the covariance characteristics of random vectors [3] evaluates the harmonic emission level using the weak correlation that occurs between the background harmonic voltage and the harmonic current measured at the PCC. However, this method cannot handle the case where filters are installed in the target harmonic source side. Based on the independence of the harmonic sources on both sides of the PCC, the complex ICA method [4,5,8] can calculate the harmonic impedances robustly. However, its reliable signal separation capacity is heavily dependent on use of a large sample size. Extension of the sampling time can increase the sample size but may also cause harmonic impedance variations and create new errors.

In fact, harmonic filters exist in numerous field cases. For example, in wind farms, harmonic filters are installed for each wind turbine. In addition, in city grids with HVDC systems, the converter stations are equipped with filters to mitigate their characteristic harmonics. In these situations, the harmonic impedance of the target harmonic source side is not much higher than that of the utility side. Therefore, conventional methods to assess the harmonic emission levels are invalid in such cases.

Complex ICA has great potential in harmonic emission level evaluation and is worthy of improvement to adapt to situations where filters are installed for the target harmonic source side. In this paper, a screening mechanism based on sparse component analysis [9,10] and maximization of the non-Gaussianity is introduced to

improve the signal separation capacity of traditional complex ICA. The improved complex ICA method proposed here is suitable for situations in which the background harmonic fluctuates considerably and the harmonic impedance amplitudes on both sides are close to each other. Simulations are conducted to verify the validity of the proposed improved complex ICA method.

HARMONIC EMISSION MODE

The harmonic model can be presented by the Norton equivalent circuit shown in Fig. 1.

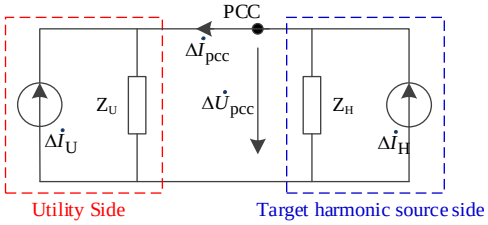

Fig.1. Norton equivalent circuit.

According to the principle of superposition, we have

$$\begin{cases} \Delta\dot{U}_{pcc} = \dfrac{Z_U Z_H}{Z_U + Z_H}\left(\Delta\dot{I}_U + \Delta\dot{I}_H\right) \\ \Delta\dot{I}_{pcc} = \dfrac{Z_H}{Z_U + Z_H}\Delta\dot{I}_H - \dfrac{Z_U}{Z_U + Z_H}\Delta\dot{I}_U \end{cases}, \tag{1}$$

where $\Delta\dot{U}_{pcc}$ and $\Delta\dot{I}_{pcc}$ are the fluctuation components of harmonic voltages and currents measured at the PCC, respectively. $\Delta\dot{I}_U$ and $\Delta\dot{I}_H$ are the fluctuation components of the harmonic sources on the two sides. The harmonic emissions of the two sides at the PCC, which are defined as $\dot{U}_{PCC\text{-}H}$ and $\dot{U}_{PCC\text{-}U}$, are:

$$\begin{cases} \dot{U}_{PCC\text{-}H} = \dfrac{Z_U Z_H}{Z_U + Z_H}\left(\dfrac{\dot{U}_{PCC}}{Z_H} + \dot{I}_{PCC}\right) \\ \dot{U}_{PCC\text{-}U} = \dot{U}_{PCC} - \dot{U}_{PCC\text{-}H} \end{cases}, \tag{2}$$

Because the target harmonic source side is parallel with a harmonic filter, the amplitude of Z_H is reduced and thus may not be much larger than Z_U. Therefore, the influence of Z_H on harmonic emission evaluation cannot be ignored. Consequently, both Z_H and Z_U must be calculated during this evaluation process. However, because most existing methods can only calculate Z_U under the assumption that the amplitude of Z_H is far higher than that of Z_U, a new evaluation method is urgently required.

IMPROVED COMPLEX ICA ALGORITHM

Traditional complex ICA method

When source signals are independent, we can separate them using complex ICA method. In Eq. (1), $\Delta\dot{I}_H$ and $\Delta\dot{I}_U$ are independent for each other [8], and we have

$$\boldsymbol{X} = \mathbf{A}\boldsymbol{S}, \tag{3}$$

where $\boldsymbol{X} = [\Delta\dot{U}_{PCC}\ \ \Delta\dot{I}_{PCC}]^T$ and $\boldsymbol{S} = [\Delta\dot{I}_U\ \ \Delta\dot{I}_H]^T$. The unknown matrix **A** is mixed by Z_U and Z_H.

Using complex ICA, the source signals, $\Delta\dot{I}_U$ and $\Delta\dot{I}_H$, can be recovered as the signals $\boldsymbol{Y}=[Y_U\ \ Y_H]$. The calculation process is presented in detail in [8] and because of space limitations, these calculations will not be repeated here. Using the separated signals $\boldsymbol{Y}$, the matrix **A** can be obtained in the form

$$\hat{\mathbf{A}} = \boldsymbol{X}\boldsymbol{Y}^T(\boldsymbol{Y}\boldsymbol{Y}^T)^{-1}. \tag{4}$$

The results of complex ICA have the uncertainty of ranking order, which means that it is unknown whether $\boldsymbol{Y} = [\dot{Y}_U\ \ \dot{Y}_H]^T$ or $\boldsymbol{Y} = [\dot{Y}_H\ \ \dot{Y}_U]^T$ is true. To solve this problem, we define

$$\begin{cases} k_1 = \hat{A}(1,1)/\hat{A}(2,1) \\ k_2 = \hat{A}(1,2)/\hat{A}(2,2) \end{cases}. \tag{5}$$

Because the resistive part of the impedance is always positive, we can distinguish $\hat{Z}_U$ and $\hat{Z}_H$ using

$$k_i = \begin{cases} \hat{Z}_U, if\ k_{i,r} > 0 \\ -\hat{Z}_H, if\ k_{i,r} < 0 \end{cases} (i = 1,2). \tag{6}$$

where $k_{i,r}$ is the resistive part of k_i. Finally, Z_U and Z_H are thus obtained.

In applications, the effects of complex ICA are heavily reliant on the amount of data available. Only the use of large amounts of data can ensure high calculation accuracy for the harmonic impedances on both sides. However, a large sample size may cause the harmonic impedance to vary and thus produce new errors. Therefore, it is necessary to improve the existing method to obtain precise results when the number of sampling points is limited. The calculation errors of the complex ICA are mainly caused by the differences between the separated signals and the true source signals. Therefore, in this paper, we focus on improving the degree of coincidence of these signals.

The improved complex ICA

To make complex ICA valid when both Z_U and Z_H must be calculated, a novel blind source separation technology called sparse component analysis (SCA) is introduced. The core idea of SCA is that when the source signals are sparse, the mixed signal $\boldsymbol{X}$ will then cluster into two straight lines. Additionally, the slopes of these two lines are equal to the harmonic impedances of the two sides. To introduce the theory for SCA, we set $[s_1\ s_2]^T$ and $[x_1\ x_2]^T$ as the source and mixed signals, respectively. Thus,

$$\begin{bmatrix} x_1 \\ x_2 \end{bmatrix} = \begin{bmatrix} a_{11} & a_{12} \\ a_{21} & a_{22} \end{bmatrix}\begin{bmatrix} s_1 \\ s_2 \end{bmatrix}. \tag{7}$$

If $[s_1\ s_2]^T$ are sparse signals, then at most times only one of these signals is nonzero. By assuming at the sampling time t_1 that $s_2(t_1)\approx 0$ and $s_1(t_1)\neq 0$, we obtain

$$\begin{cases} x_1(t_1) = a_{11}s_1(t_1) \\ x_2(t_1) = a_{21}s_1(t_1) \end{cases}. \tag{8}$$

Therefore,

$$x_1(t_1)/x_2(t_1)=a_{11}/a_{21} \quad (9)$$

Similarly, at sampling t_2, if $s_1(t_2)\approx 0$ and $s_2(t_2)\neq 0$, we have

$$x_1(t_2)/x_2(t_2)=a_{12}/a_{22} \quad (10)$$

By combining Eqs. (5)–(10), we can see that when the source signals are sparse, the mixed signals $\boldsymbol{X}$ will cluster into two lines with slopes of Z_U and Z_H, respectively.

However, in practice, most source signals are not sparse. Therefore, before performing the SCA, the source signals require pre-sparse processing. Using the sparse dictionary transformation process [9,10], a signal s can be sparse as

$$s^{\mathrm{T}}=\mathbf{D}\left(s^{\mathbf{D}}\right)^{\mathrm{T}} \Rightarrow s^{\mathbf{D}}=s\left(\mathbf{D}^{-1}\right)^{\mathrm{T}}, \quad (11)$$

where the full rank matrix $\mathbf{D}$ is the sparse dictionary of s. The dimension of $\mathbf{D}$ is the same as the length of s. The signal $s^{\mathbf{D}}$ is the sparse signal that corresponds to s. Using the sparse dictionary transformation in Eq. (3), we obtain

$$\boldsymbol{X}\left(\mathbf{D}^{-1}\right)^{\mathrm{T}}=\mathbf{A}\boldsymbol{S}\left(\mathbf{D}^{-1}\right)^{\mathrm{T}}, \quad (12)$$

which means that this transformation will not change matrix $\mathbf{A}$. Because the source signals $\boldsymbol{S}(\mathbf{D}^{-1})^{\mathrm{T}}$ are sparse, the mixed signals $\boldsymbol{X}(\mathbf{D}^{-1})^{\mathrm{T}}$ cluster linearly and we can calculate Z_U and Z_H based on their slopes.

Generally, signals can be made sparse by converting them from the time domain to the frequency domain. Therefore, the sparse dictionary $\mathbf{D}$ can be obtained via wavelet packet or short-time Fourier transform (STFT)-based transformations [9,10]. However, for source signals that contain rich frequency information, e.g., $\Delta\dot{I}_U$ and $\Delta\dot{I}_H$, the sparse effects of these transformations are unsatisfactory [11]. Therefore, in this paper, SCA is not used to calculate Z_U and Z_H directly but is used to improve the complex ICA method. The improvement measures are described in detail as follows.

The main idea of this novel method is to search around the signals that are separated from the complex ICA to determine the local signals, which are highly consistent with the true harmonic source signals. Then, the harmonic impedances of both sides can be calculated using these local signals. The calculation of Z_U is used here as an example to show how to achieve these results and the same calculation process is used for Z_H. First, we define $\dot{y}_{\mathrm{u},i}$ is the ith local signals searching around Y_U. The signal $\Delta\dot{I}_{\mathrm{U},i}$ is the true local source signal corresponding to the sampling time of $\dot{y}_{\mathrm{u},i}$, while x_i is the corresponding local mixed signals. During the search process, SCA is used to construct a screening criterion to identify these local signals.

By solving Eq. (13), $\dot{y}_{\mathrm{u},i}$ can be made sparse and its corresponding sparse dictionary $\mathbf{D}_i$ can then be obtained:

$$\min_{\boldsymbol{D}_i,\dot{y}_{\mathrm{u},i}^{\mathbf{D}}}\left\{\left\|\left(\dot{y}_{\mathrm{u},i}\right)^{\mathrm{T}}-\boldsymbol{D}_i\left(\dot{y}_{\mathrm{u},i}{}^{\mathbf{D}}\right)^{\mathrm{T}}\right\|_2^2\right\} \text{ s.t. } \left\|\dot{y}_{\mathrm{u},i}{}^{\mathbf{D}}\right\|_0\le \mathrm{T}_0, \quad (13)$$

where $\dot{y}_{\mathrm{u},i}{}^{\mathbf{D}}$ represents the sparse signals. T_0 is the degree of sparsity, i.e., the number of nonzero elements in $\dot{y}_{\mathrm{u},i}{}^{\mathbf{D}}$. The symbols $\|\ \|_2$ and $\|\ \|_0$ represent the two-norm and the zero-norm of the signal, respectively.

Equation (13) can be solved using the KSVD algorithm presented in [12]. While the true local source signal $\Delta\dot{I}_{\mathrm{U},i}$ is unknown, we can still assess the degree of coincidence between the local signal $\dot{y}_{\mathrm{u},i}{}^{\mathbf{D}}$ and $\Delta\dot{I}_{\mathrm{U},i}$ using the SCA method. By using the sparse dictionary $\mathbf{D}_i$ of $\dot{y}_{\mathrm{u},i}{}^{\mathbf{D}}$, x_i can be transformed into $x_i\ (\boldsymbol{D}_i^{-1})^{\mathrm{T}}$ and there are then two possible results, which are described as follows:

1) $\dot{y}_{\mathrm{u},i}$ coincides with $\Delta\dot{I}_{\mathrm{U},i}$:

At this time, $\mathbf{D}_i$ can make the true source signal $\Delta\dot{I}_{\mathrm{U},i}$ sparse, and thus $x_i\ (\boldsymbol{D}_i^{-1})^{\mathrm{T}}$ will cluster into a straight line with a slope equal to Z_U.

2) $\dot{y}_{\mathrm{u},i}$ does not coincide with $\Delta\dot{I}_{\mathrm{U},i}$:

In this case, $\mathbf{D}_i$ cannot make $\Delta\dot{I}_{\mathrm{U},i}$ sparse. We define $\Delta\dot{I}_{\mathrm{U},i}{}^{\mathbf{D}}=\Delta\dot{I}_{\mathrm{U},i}\left(\boldsymbol{D}_i^{-1}\right)^{\mathrm{T}}$, $\Delta\dot{I}_{\mathrm{H},i}{}^{\mathbf{D}}=\Delta\dot{I}_{\mathrm{H},i}\left(\boldsymbol{D}_i^{-1}\right)^{\mathrm{T}}$, and signals $x_i\ (\boldsymbol{D}_i^{-1})^{\mathrm{T}}$ can cluster into a line only when Eq. (14) hold, which is of little chance [10].

$$\frac{\Delta\dot{I}^{\mathbf{D}}_{\mathrm{U},i,1}}{\Delta\dot{I}^{\mathbf{D}}_{\mathrm{H},i,1}}=\frac{\Delta\dot{I}^{\mathbf{D}}_{\mathrm{U},i,2}}{\Delta\dot{I}^{\mathbf{D}}_{\mathrm{H},i,2}}=\ldots=\frac{\Delta\dot{I}^{\mathbf{D}}_{\mathrm{U},i,n\text{-}\mathrm{T0}}}{\Delta\dot{I}^{\mathbf{D}}_{\mathrm{H},i,n\text{-}\mathrm{T0}}}, \quad (14)$$

where n is the length of the true local source signals. T_0 is the degree of sparsity for $\dot{y}_{\mathrm{u},i}{}^{\mathbf{D}}$. The subscripts 1, 2, and n-T_0 represent the sampling point where $\dot{y}_{\mathrm{u},i}{}^{\mathbf{D}}$ is zero.

Therefore, by defining $x_i^{\mathbf{D}}=x_i\left(\boldsymbol{D}_i^{-1}\right)^{\mathrm{T}}$, we can use the linear clustering degree of $x_i^{\mathbf{D}}$ as a criterion to identify whether or not $\dot{y}_{\mathrm{u},i}$ and $\Delta\dot{I}_{\mathrm{U},i}$ coincide. The specific criterion is presented in Eq. (15).

$$\begin{cases}\sigma_{sparse}=\max\left(\left|\dfrac{x_i^{\mathbf{D}}{}_{1,j}}{x_i^{\mathbf{D}}{}_{2,j}}-\dfrac{x_i^{\mathbf{D}}{}_{1,k}}{x_i^{\mathbf{D}}{}_{2,k}}\right|\right),\forall j\neq k\\ \sigma_{sparse}<\varepsilon\end{cases}, \quad (15)$$

where σ_{sparse} is the sparse screening index. The subscripts 1 and 2 represent the first and second lines of $x_i^{\mathbf{D}}$, respectively. The symbols j and k represent the sampling points where $\dot{y}_{\mathrm{s},i}{}^{\mathbf{D}}$ is zero. The symbol ε represents the sparse screening threshold.

If Eq. (15) holds, it can then be considered that $\dot{y}_{\mathrm{u},i}{}^{\mathbf{D}}$ coincides with $\Delta\dot{I}_{\mathrm{U},i}$. The harmonic impedance of the utility side can then be calculated using

$$\hat{\mathrm{Z}}_{\mathrm{U},i}=\frac{1}{n-\mathrm{T}_0}\sum_{j=1}^{n-\mathrm{T}_0}\frac{x_i^{\mathbf{D}}{}_{1,j}}{x_i^{\mathbf{D}}{}_{2,j}} \quad (16)$$

During the search process, the length of the local signal $\dot{y}_{\mathrm{u},i}$ should be as short as possible to reduce the searching dimension. However, if its length is less than 3, Eq. (15) will always hold for any signal. We thus set the length of $\dot{y}_{\mathrm{s},i}$ to be 3. The dimensions of $\mathbf{D}_{\mathrm{u},i}$ are thus 3×3.

The search process can be completed by exhaustive searching around $\dot{Y}_{\mathrm{U}}$ or using an intelligent optimization algorithm (e.g., particle swarm optimization) with the objective of minimizing σ_{sparse}. In the same way, we can also calculate $\hat{\mathrm{Z}}_{\mathrm{H},i}$ for the target harmonic source side.

While the possibility that Eq. (14) will hold is low, it may cause the sparse screening mechanism to be less than absolutely reliable. Among the local signals that are searched out using Eq. (15), some are highly consistent with the true source signals, but a few of these signals are searched wrongly. Therefore, to make this method more robust, we screen these local signals once again according to their non-Gaussianity.

When the non-Gaussianity of a complex signal that has been separated from the complex ICA is strong, the real and imaginary parts that are decomposed from the complex signal also have strong non-Gaussianity [4]. When the calculation results have low precision, the non-Gaussianity of both the real and imaginary parts of the separated signal is weak. Therefore, the non-Gaussianity of the real and imaginary parts of the calculated signals can be set as an index for a secondary screening.

First, we should calculate $\dot{y}_{\mathrm{U},i}^{\mathrm{global}}$ and $\dot{y}_{\mathrm{H},i}^{\mathrm{global}}$, which are the global signals corresponding to $\dot{y}_{\mathrm{U},i}$ and $\dot{y}_{\mathrm{H},i}$, respectively, using Eq. (17).

$$\begin{bmatrix} \dot{y}_{\mathrm{h},i}^{\mathrm{global}} \\ \dot{y}_{\mathrm{u},i}^{\mathrm{global}} \end{bmatrix} = \begin{bmatrix} 1/\hat{\mathrm{Z}}_{\mathrm{H},i} & 1 \\ 1/\hat{\mathrm{Z}}_{\mathrm{U},i} & -1 \end{bmatrix} \begin{bmatrix} \Delta\dot{U}_{\mathrm{PCC}} \\ \Delta\dot{I}_{\mathrm{PCC}} \end{bmatrix}. \tag{17}$$

where $\hat{\mathrm{Z}}_{\mathrm{U},i}$ and $\hat{\mathrm{Z}}_{\mathrm{H},i}$ are the harmonic impedances calculated from $\dot{y}_{\mathrm{u},i}$ and $\dot{y}_{\mathrm{h},i}$. Additionally, the lengths of $\dot{y}_{\mathrm{u},i}^{\mathrm{global}}$ and $\dot{y}_{\mathrm{h},i}^{\mathrm{global}}$ are the same as that of $\dot{I}_{\mathrm{U}}^{\mathrm{fast}}$.

For the local signals $\dot{y}_{\mathrm{u},i}$ or $\dot{y}_{\mathrm{h},i}$ that satisfy Eq. (15), we can calculate the corresponding global signals $\dot{y}_{\mathrm{u},i}^{\mathrm{global}}$ and $\dot{y}_{\mathrm{h},i}^{\mathrm{global}}$, respectively, and screen the signal with the largest non-Gaussianity. Therefore, the corresponding harmonic impedance is the final result. The non-Gaussianity of an arbitrary signal s can be assessed through kurtosis:

$$\sigma_{\mathrm{kurt}}(s) = \mathrm{E}\left[s^4\right] - 3(\mathrm{E}\left[s^2\right])^2. \tag{18}$$

Higher absolute values of $\sigma_{\mathrm{kurt}}(s)$ correspond to better non-Gaussianity for s. The non-Gaussianity evaluation index can be constructed by normalizing and averaging the absolute values of the kurtosis for the real and imaginary components of $\dot{y}_{\mathrm{u},i}^{\mathrm{global}}$ and $\dot{y}_{\mathrm{h},i}^{\mathrm{global}}$.

Consequently, based on the proposed sparse screening and non-Gaussianity secondary screening sequence, we can obtain both $\hat{\mathrm{Z}}_{\mathrm{U},i}$ and $\hat{\mathrm{Z}}_{\mathrm{H},i}$ accurately.

SIMULATION ANALYSIS

To compare the calculation errors for each method, simulation data were set. Then, the PCC data, including 15000 sample points, are generated.

1) Harmonic current sources: the amplitude and the phase angle of $\dot{I}_{\mathrm{H}}$ are set at 100 A and −30 °, respectively. The amplitude of $\dot{I}_{\mathrm{U}}$ is k times that of $\dot{I}_{\mathrm{H}}$. The phase angle of $\dot{I}_{\mathrm{U}}$ is set at −30 °. The amplitude and the phase angle for both $\dot{I}_{\mathrm{H}}$ and $\dot{I}_{\mathrm{U}}$ have ±10% sine fluctuations and ±5% random disturbances added.

2) Harmonic impedances: set $\mathrm{Z_U}$=5+12j Ω. For harmonic source side, given that, its harmonic impedance may be reduced for installation of the harmonic filters, we set $\mathrm{Z_H}$=8+30j Ω. ±10% sine fluctuations are added with them. The 15000 simulation data are divided into 100 segments for the simulation. Four methods, i.e., 1) the binary linear regression method; 2) the covariance characteristic method; 3) complex ICA; and 4) the proposed improved complex ICA, are used to calculate $\mathrm{Z_U}$. Because most of the existing methods cannot calculate $\mathrm{Z_H}$, the calculation errors for $\mathrm{Z_H}$ can only be compared using the complex ICA and the proposed method. The average errors for each of the methods are shown in Fig. 2.

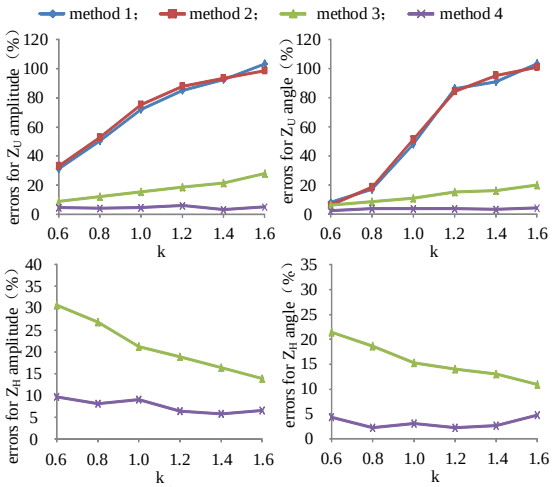

Fig.2. Average errors of $\mathrm{Z_U}$ and $\mathrm{Z_H}$

Fig. 2 shows that there are large errors in methods 1 and 2, and these errors increase rapidly with increasing background harmonics. The reason for this is that method 1 is only suitable for cases with stable background harmonics. While method 2 can reduce the effects of the background harmonic fluctuations, the necessary condition, i.e., $|\mathrm{Z_H}|>>|\mathrm{Z_U}|$, does not hold in this case. When compared with methods 1 and 2, the results from method 3 are improved but are not satisfactory either. Because the amplitudes of $\mathrm{Z_H}$ and $\mathrm{Z_U}$ are close, the errors remain serious and the errors of $\mathrm{Z_U}$ increase with increasing background harmonics. However, reduction of the background harmonics causes the errors of $\mathrm{Z_H}$ to increase. By comparison, when using the screening mechanism based on SCA and non-Gaussianity, the proposed method can calculate the harmonic impedances

for both sides accurately.

The core of the proposed method is searching for the signals that are highly coincident with the true harmonic source to improve the accuracy of the impedance calculations. To further validate the method, we used calculation of the utility side as an example, and the source signal separation results for each method for k=1.6 are shown in Fig. 3. It is obvious from the results that the signal separation effects of complex ICA are unsatisfactory. In comparison, the proposed method can find the signals that have a high degree of similarity with the true source signals.

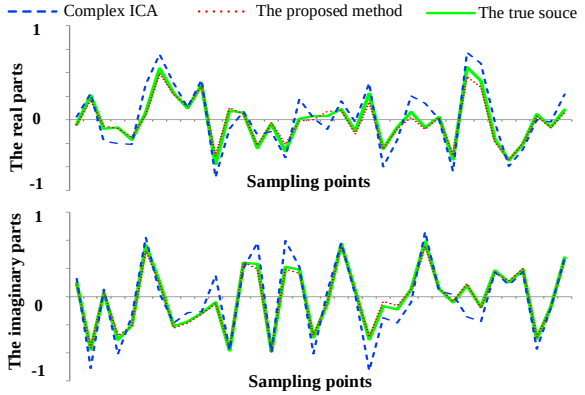

Fig.3. The signal separation capacity of the two methods.

As previously analyzed, the key of evaluating harmonic emission levels for both sides at the PCC is calculating their harmonic impedances precisely. Thus, since the proposed method can calculate harmonic impedances accurately, it can be concluded that, our method can precisely evaluate harmonic emission levels even when the target harmonic source side are equipped with filters.

CONCLUSION

In this paper, we study the harmonic emission level evaluation method and aim at the situations where filters are installed in the target harmonic source side. The main contributions are as follows.

1) The signal separation capacity of the traditional complex ICA is improved by introduction of a screening mechanism based on sparse component analysis and maximization of the non-Gaussianity.

2) When the target harmonic source side has harmonic filters installed, the corresponding harmonic impedance may not be much larger than that of the utility side, which leads to failure of the traditional harmonic emissions evaluation method. In contrast, the proposed method can calculate the harmonic impedance for both sides precisely and also obtains accurate evaluation results.

The technique enhancing the searching efficiency for this algorithm will be further studied in the future.

Acknowledgments

This paper is supported by The State Grid Corporation of China Research Program (SGSHDK00DWJS1800225).

REFERENCES

[1] Bozicek A, Kilter J, Sarnet T, et al, 2018, "Harmonic emissions of power-electronic devices in different transmission-network operating conditions", *IEEE Transactions on Industry Applications*. vol. 54, 5216 - 5226.

[2] Hui J, Freitas W, Vieira J C M , et al, 2012, "Utility harmonic impedance measurement based on data selection", *IEEE Transactions on Power Delivery*. vol. 27, 2193–2203.

[3] Hui J, Yang H, Lin S, et al, 2010, "Assessing utility harmonic impedance based on the covariance characteristic of random vectors", *IEEE Transactions on Power Delivery*. vol. 25, 1778–1786.

[4] Zhao X, Yang H, 2016, "A New Method to Calculate the Utility Harmonic Impedance Based on FastICA", *IEEE Transactions on Power Delivery*. vol. 31, 381–388.

[5] Karimzadeh F, Esmaeili S, Hosseinian S H, 2016, "A novel method for noninvasive estimation of utility harmonic impedance based on complex independent component analysis", *IEEE Transactions on Power Delivery*. vol. 30, 1843-1852.

[6] Honggeng Yang, P Porotte, A Robert, 1994, "Assessing the harmonic emission level from one particular customer", *Proceedings of the 3rd International Conference on Power Quality Proceedings*, vol.2, 160-166.

[7] Yonghai, Xu, Huang Shun, and Liu Yingying, 2006, "Partial Least-Squares Regression Based Harmonic Emission Level Assessing at the Point of Common Coupling", *International Conference on Power System Technology IEEE*, 1-5.

[8] Karimzadeh F, Hossein Hosseinian S, Esmaeili S, 2016, "Method for determining utility and consumer harmonic contributions based on complex independent component analysis", *Generation Transmission & Distribution IET*. vol. 10, 526-534.

[9] Yu Xianchuan, Xu Jindong, Hu Dan, and Xing Haihua, 2013, "A new blind image source separation algorithm based on feedback sparse component analysis", *Signal Processing*. vol. 93, 288-296.

[10] V.G. Reju, Soo Ngee Koh, and Ing Yann Soon, 2009, "An algorithm for mixing matrix estimation in instantaneous blind source separation", *Signal Processing*. vol. 89, 1762-1773.

[11] Abolghasemi Vahid, Ferdowsi Saideh, and Sanei Saeid, 2012, "Blind Separation of Image Sources via Adaptive Dictionary Learning", *IEEE Transactions on Image Processing*. vol. 21, 2921-2930.

[12] Aharon M, Elad M, et al, 2006, "K-SVD: An Algorithm for Designing Overcomplete Dictionaries for Sparse Representation", *IEEE Transactions on Signal Processing*. vol. 54, 4311-4322.